

# Pitch Guidance Optimization for the Orion Abort Flight Tests

Ryan A. Stillwater<sup>1</sup>

*NASA Dryden Flight Research Center, Edwards, California, 93523*

The National Aeronautics and Space Administration created the Constellation program to develop the next generation of manned space vehicles and launch vehicles. The Orion abort system is initiated in the event of an unsafe condition during launch. The system has a controller gains schedule that can be tuned to reduce the attitude errors between the simulated Orion abort trajectories and the guidance trajectory. A program was created that uses the method of steepest descent to tune the pitch gains schedule by an automated procedure. The gains schedule optimization was applied to three potential abort scenarios; each scenario tested using the optimized gains schedule resulted in reduced attitude errors when compared to the Orion production gains schedule.

## Nomenclature

AFT	Abort Flight Test
ACM	Attitude Control Motor
AM	Abort Motor
ANTARES	Advanced NASA Technology Architecture for Exploration Studies
ATB	Abort Test Booster
$c$	bias value applied to $\bar{z}$
CM	Crew Module
$C_{p,\beta}$	aerodynamic roll moment coefficient with respect to $\beta$
$f$	function
$g$	sum of the square of the angle of attack errors
$h$	coefficient for Newton's Forward Divided Difference Formula
$j$	inner loop iteration number
$\bar{J}$	Jacobian matrix
JM	Jettison Motor
$\bar{K}$	gains array
$K_q$	pitch rate gain
$K_\alpha$	angle of attack gain
$K_{i\alpha}$	integral angle of attack gain
$K_\gamma$	flight path angle gain
$K_\theta$	pitch angle gain
LAS	Launch Abort System
LAV	Launch Abort Vehicle
NASA	National Aeronautics and Space Administration
$n$	outer-loop iteration number
$p$	roll rate
$q$	pitch rate
$r$	yaw rate

---

<sup>1</sup> Aerospace Engineer, Dynamics and Controls Branch, P.O. Box 273, Mail Stop 4830-B, AIAA Member.

$\bar{z}$	normalized gradient of $g$
$\alpha$	angle of attack
$\alpha_e$	angle of attack error
$\beta$	angle of sideslip
$\gamma$	flight path angle
$\Delta$	difference
$\delta$	partial differential
$\theta$	pitch angle
$P$	Newton's Forward Divided Difference Formula
$\sigma$	standard deviation
$\varphi$	roll angle
$\psi$	yaw angle

## I. Introduction

The National Aeronautics and Space Administration (NASA) created the Constellation program to develop the next generation of manned space vehicles and launch vehicles. The NASA vision for the next manned spaceflight vehicle, known as Orion, involves a return to the capsule configuration similar to that used for Mercury, Gemini, and Apollo. The Orion vehicle will be taken into orbit by the Ares I launch vehicle.

The Orion abort system is initiated in the event of an unsafe condition during launch. The gains schedule of the Orion Launch Abort System (LAS) can be tuned to reduce the error between the angle of attack,  $\alpha$ , of the simulated Orion abort trajectories and the desired  $\alpha$  schedule. A program was created that uses the method of steepest descent to tune the gains schedule by an automated procedure.

### A. Concept of Operations

Figure 1 shows a visual representation of the sequence of events during an aborted launch. The Orion abort system first ignites a set of solid rocket motors to separate the Orion capsule from the Ares I booster. During the ascent phase of the abort sequence, the attitude of the Orion capsule is commanded to follow a guidance schedule. A second set of solid rocket motors uses the guidance commands to control the Orion capsule. Once reorientation conditions have been reached, the second set of solid rocket motors reorients the Orion capsule from the heat-shield-aft (ascent) orientation to the heat-shield-forward (entry) orientation. Once reorientation has been completed, a third set of solid rocket motors separates the LAS from the Orion capsule. Lastly, the parachute sequence begins and slows the Orion capsule to its landing velocity.

### B. System Description

Figure 2<sup>1</sup> shows the Orion vehicle breakdown and naming convention. The Orion vehicle consists of four main sections: the spacecraft adapter, the service module, the Crew Module (CM), and the LAS. During an aborted launch, the LAS and the CM remain connected throughout the ascent and reorientation phases; this combination comprises the Launch Abort Vehicle (LAV).

The LAS consists of three solid rocket motors that work in tandem to ensure that the CM safely separates from the booster: the Abort Motor (AM), the Attitude Control Motor (ACM), and the Jettison Motor (JM). During an aborted launch, the LAS first ignites the AM and the ACM. The AM is located near the base of the LAS and is a solid rocket motor with four reverse-flow nozzles. The AM is a high-thrust motor that separates the CM from the Ares I. The ACM is located at the top of the LAS and is a solid rocket motor with eight thrust-varying nozzles. The ACM provides attitude control during the ascent phase of the abort trajectory and reorients the LAV into a heat-shield-forward position. Approximately 27 s after abort initiation, the JM ignites and separates the LAS from the CM. The JM, located between the AM and the ACM, is a solid rocket with four direct-flow nozzles.

The AM, ACM, and JM are controlled by the LAS controller, which was developed by Orbital Sciences Corporation (Dulles, Virginia, USA). The LAS controller is a proportional-integral-derivative controller with individual channels for the pitch and yaw axes. The LAS controller calculates the error between the current vehicle attitude and rates, and the guidance attitude and rates, to input into the channels. The controller gains are calculated from a one-dimensional gains schedule table based on the time since abort. The gains are combined with vehicle attitude errors and rate errors to generate the commands. Figure 3 shows the block diagram for the pitch channel of

the LAS controller. The inputs to the pitch channel are the errors from  $\alpha$ ; the pitch angle,  $\theta$ ; the pitch rate,  $q$ ; and the flight path angle,  $\gamma$ .

The inputs to the yaw channel are the errors from the angle of sideslip,  $\beta$ ; the yaw angle,  $\psi$ ; the yaw rate,  $r$ ; the roll angle,  $\phi$ ; the roll rate,  $p$ ; and the heading. The yaw channel uses a gains schedule and the errors between the inputs and the reference values to control the LAV to the desired  $\beta$  profile. The yaw channel uses the vehicle  $\phi$  and  $p$  because it also commands a  $\beta$  to generate an aerodynamic roll moment from the  $C_{p,\beta}$  aerodynamic coefficient. This roll moment damps out the  $p$  imparted to the LAV from the booster. Adjusting the gains of the yaw channel would also affect the roll dampening efforts; the gains schedule tuning discussed in this paper is limited to that concerning the pitch channel.

### C. Flight Test Overview

The Flight Test Office of the Constellation program is located at the NASA Dryden Flight Research Center, Edwards, California, USA, and has been tasked with demonstrating the LAS capability in a series of Abort Flight Tests (AFTs). The AFTs originally consisted of two abort tests from the launch pad (pad aborts) and four abort tests at various stages along the Orion operational trajectory (ascent aborts). The gains schedule tuning efforts were focused on the ascent aborts. The first ascent abort scenario was designed to test the minimum force required to separate the LAV from the Ares I and was targeting the transonic region of the operational trajectory. The second ascent abort scenario was designed to stress the structural dynamic loads of the LAV by targeting the maximum dynamic pressure region of the operational trajectory. The third ascent abort scenario was also at the maximum dynamic pressure region of the operational trajectory, but was designed to further stress the structural dynamic loads of the LAV by simulating a failure scenario in which the actuators of the Ares I stage 1 nozzle moved to a hard-over condition and stopped responding. The final ascent abort scenario targeted the stage 1 to stage 2 transition region of the operational trajectory in order to demonstrate LAV aborts from the pad up through the LAV abort to abort-to-orbit transition point. The first three ascent abort scenarios were scheduled to be conducted at the United States Army White Sands Missile Range (Las Cruces, New Mexico, USA) and to use an Abort Test Booster (ATB) to be supplied by Orbital Sciences Corporation (Chandler, Arizona, USA) to take the LAV to the desired test condition. The stage 1 to stage 2 transition region scenario was scheduled to be conducted at the NASA Kennedy Space Center (Kennedy Space Center, Florida, USA) and to use an operational Ares I launch vehicle to take the LAV to the desired test condition.

### D. Simulation Overview

Prior to the execution of a flight test, the entire test is modeled in a simulated environment. The LAV simulation discussed in this paper is the Advanced NASA Technology Architecture for Exploration Studies (ANTARES) simulation developed by NASA. The ANTARES simulation can create variety of specific Orion missions by modifying the initial vehicle state variables, mass properties, aerodynamic coefficients, et cetera. The simulated Orion mission can be generated as an individual run or in a dispersed Monte Carlo set. The gains schedule tuning program loads the vehicle state data from an ANTARES-simulated Orion mission and calculates a revised gains schedule. The same ANTARES-simulated Orion mission is then re-run using the revised gains schedule to generate new vehicle state data. The process is repeated until the gains schedule tuning program converges on a solution.

Orbital Sciences Corporation (Chandler, Arizona, USA) has developed a simulation of the ATB/LAV trajectory that targets the transonic and maximum dynamic pressure regions of the Orion/Ares I operational trajectory. When the ATB/LAV reaches the desired test condition, a signal is sent to the LAV to begin the ATB/LAV separation sequence. The LAV separation point can occur at a variety of positions, velocities, attitudes, attitude rates, and atmospheric conditions. The conditions of the ATB simulation at the LAV separation points are the initial conditions of the LAV simulation in ANTARES.

## II. Problem Statement

The gains schedule of the production Orion abort system is tuned to account for the possibility of an abort from on the pad up through orbit. The Orion ascent AFTs focus on a small subset of the Orion trajectory. The Orion production gains schedule needs to be re-tuned for each individual scenario; this will reduce the error between the AFT-dispersed simulated trajectories and the desired attitude profile. The standard abort trajectory profile commands zero  $\alpha$  and  $\beta$  from LAV separation until reorientation. In order to not interfere with the  $\beta$ -commanded roll rate control, the abort trajectory profile targeting is limited to the pitch channel only. The AFT gains schedule

must have the capability to handle the variety of LAV separation conditions provided by the ATB simulation. Only the ATB flight tests were analyzed due to the lack of focused initial conditions from the ATB simulation for the stage 1 to stage 2 transition scenario. The metric for how well the AFT gains schedule perform was how well the dispersed trajectories approximate the desired  $\alpha$  profile.

### III. Cost Function

The difference between the desired  $\alpha$  and the resulting  $\alpha$  is the  $\alpha$  error,  $\alpha_e$ . The  $\alpha_e$  is the cost to be minimized in this optimization and varies based on the LAS controller gains that are used in the simulation run. The same scenario can be run with different gains schedule, which results in a different  $\alpha_e$ . This is expressed as the cost function shown in Eq. 1, with  $\alpha_e$  as a dependent variable and the LAS controller gains as the independent variables.

$$\alpha_e = f(K_\alpha, K_{i\alpha}, K_q, K_\theta, K_\gamma) \quad (1)$$

The controller gains used in the pitch channel are the  $\alpha$  gain ( $K_\alpha$ ), the integral  $\alpha$  gain ( $K_{i\alpha}$ ), the q gain ( $K_q$ ), the  $\theta$  gain ( $K_\theta$ ), and the  $\gamma$  gain ( $K_\gamma$ ). The integral  $\alpha$  error, q error,  $\theta$  error, and  $\gamma$  error are also dependent variables to Eq. 1, but the  $\alpha_e$  is the only dependent variable that is minimized in this study.

The  $\alpha_e$  will be minimized at a series of 31 linearly-spaced time points along the pre-reorientation region of the abort trajectory. The optimal solution for the ascent abort gains schedule is at the minima of the non-linear, multivariable function expressed in Eq. (1). To solve for the minima of this multivariable problem the method of steepest descent<sup>2</sup> is used. The method of steepest descent converges where the gradient of Eq. (1) is equal to zero.

### IV. Method of Gains Optimization

The gains schedule optimization is divided into an outer loop and an inner loop. The outer loop calculates the computationally intensive Jacobian matrix that is carried thru the inner loop iterations. The inner loop uses the method of steepest descent<sup>2</sup> to optimize the gains schedule for each of the 31 time points. Before starting the next outer loop iteration, the gradient of Eq. (1) is checked against a preset tolerance value to determine in the system has converged.

#### A. Outer Loop

The outer loop is used to calculate the Jacobian matrix, Eq. (2), and it is assumed that the Jacobian matrix does not change significantly in the inner loop. The partial derivatives of Eq. (2) are not known due to the inherent variability in the simulated vehicle dynamics. The Jacobian matrix can be approximated by varying the gains individually and using a mid-point Taylor series derivative, Eq. (3).

$$\overline{K}_{n,1} = \begin{bmatrix} K_{\alpha_{n,1}} \\ K_{i\alpha_{n,1}} \\ K_{q_{n,1}} \\ K_{\theta_{n,1}} \\ K_{\gamma_{n,1}} \end{bmatrix}$$

$$\bar{J}(\overline{K_{n,1}}) = \begin{bmatrix} \frac{\delta f}{\delta K_{\alpha_{n,1}}} \\ \frac{\delta f}{\delta K_{i\alpha_{n,1}}} \\ \frac{\delta f}{\delta K_{q_{n,1}}} \\ \frac{\delta f}{\delta K_{\theta_{n,1}}} \\ \frac{\delta f}{\delta K_{\gamma_{n,1}}} \end{bmatrix} \quad (2)$$

$$\begin{aligned} \overline{K_{n,1}} + \Delta K_{\alpha} &= \begin{bmatrix} K_{\alpha_{n,1}} \\ K_{i\alpha_{n,1}} \\ K_{q_{n,1}} \\ K_{\theta_{n,1}} \\ K_{\gamma_{n,1}} \end{bmatrix} + \begin{bmatrix} \Delta K_{\alpha} \\ 0 \\ 0 \\ 0 \\ 0 \end{bmatrix}, \quad \overline{K_{n,1}} - \Delta K_{\alpha} = \begin{bmatrix} K_{\alpha_{n,1}} \\ K_{i\alpha_{n,1}} \\ K_{q_{n,1}} \\ K_{\theta_{n,1}} \\ K_{\gamma_{n,1}} \end{bmatrix} - \begin{bmatrix} \Delta K_{\alpha} \\ 0 \\ 0 \\ 0 \\ 0 \end{bmatrix} \\ \frac{\delta f}{\delta K_{\alpha_{n,1}}} &\approx \frac{f(\overline{K_{n,1}} + \Delta K_{\alpha}) - f(\overline{K_{n,1}} - \Delta K_{\alpha})}{2\Delta K_{\alpha}} \end{aligned} \quad (3)$$

The formula in Eq. (3) is representative of the partial derivatives for  $\frac{\delta f}{\delta K_{i\alpha_{n,1}}}$ ,  $\frac{\delta f}{\delta K_{q_{n,1}}}$ ,  $\frac{\delta f}{\delta K_{\theta_{n,1}}}$ , and  $\frac{\delta f}{\delta K_{\gamma_{n,1}}}$  with the  $\Delta$  applied to the relevant gain.

## B. Inner Loop

Once the Jacobian matrix is approximated, the program enters the inner loop and steps through the 31 points along the gains schedule. The method of steepest descent requires that the simulation be run at least three times for each of the inner-loop iterations. The inner loop starts by running the simulation with the previous gains schedule and summing of the squares of the  $\alpha$  errors, Eq. (4).

$$\begin{aligned} c_0 &= 0 \\ \alpha_{e_0} &= f(\overline{K_{n,j}}) \\ g_0 &= \sum_{m=1}^{m=31} [\alpha_{e_0}]^2 \end{aligned} \quad (4)$$

Next, the gradient of  $g_0$  is calculated, Eq. (5):

$$\nabla g_0 = 2 * \bar{J}(\overline{K_{n,1}}) * \alpha_{e_0} \quad (5)$$

The gradient in Eq. (5) is then normalized into a unit vector, Eq. (6):

$$\bar{z} = \frac{\nabla g_0}{\|\nabla g_0\|} \quad (6)$$

The gradient unit vector,  $\bar{z}$ , is used to calculate the additional values of  $g$  needed in the method of steepest descent. The simulation is re-run with the adjusted gain settings:

$$c_2 = 1$$

$$\alpha_{e_2} = f(\overline{K_{n,j}} - c_2 * \bar{z}) \quad (7)$$

$$g_2 = \sum_{m=1}^{m=31} [\alpha_{e_2}]^2$$

The results of  $g_2$  are compared to  $g_0$ . If  $g_2$  is greater than  $g_0$ , then  $c_2$  is bisected and re-run until  $g_2$  is less than  $g_0$  or a tolerance value is reached. Once a value of  $c_2$  resulting in a  $g_2$  less than  $g_0$  is located, then  $c_2$  is again bisected and the simulation is re-run with the settings shown in Eq. (8):

$$c_1 = c_2 / 2$$

$$\alpha_{e_1} = f(\overline{K_{n,j}} - c_1 * \bar{z}) \quad (8)$$

$$g_1 = \sum_{m=1}^{m=31} [\alpha_{e_1}]^2$$

The values of  $c_0$ ,  $c_1$ , and  $c_2$  and  $g_0$ ,  $g_1$ , and  $g_2$  are then used to calculate the coefficients for the Newton's forward divided difference formula, Eq. (9):

$$h_0 = \frac{g_1 - g_0}{c_1 - c_0} \quad h_1 = \frac{g_2 - g_1}{c_2 - c_1} \quad h_2 = \frac{h_1 - h_0}{c_2 - c_0} \quad (9)$$

The values of  $h_0$ ,  $h_1$ , and  $h_2$  are the coefficients of the Newton's forward divided difference formula, Eq. (10) and Eq. (11):

$$P(c_3) = g_0 + h_0 * c_3 + h_2 * c_3 * (c_3 - c_1) \quad (10)$$

$$P'(c_3) = h_0 + 2 * h_2 * c_3 - c_1 * h_2 \quad (11)$$

Solving Eq. (11) for  $P'(c_3) = 0$  results in the next inner loop iteration starting point, Eq. (12):

$$c_3 = \frac{c_1 * h_2 - h_0}{2 * h_2} \quad (12)$$

$$\overline{K_{n,j+1}} = \overline{K_{n,j}} - c_3 * \bar{z}$$

The inner loop then begins the next iteration and moves to focus on the next point in the gains schedule. Once the inner loop reaches the last point in the gains schedule, the gradient of  $g_0$  from the final inner-loop iteration is compared to a tolerance value. If the gradient of  $g_0$  is less than the tolerance value, then the program exits. If the gradient of  $g_0$  is greater than the tolerance value, then the gains schedule from the final inner-loop iteration becomes the starting point for the next outer-loop iteration, Eq. (13).

$$\overline{K_{n+1,1}} = \overline{K_{n,j+1}} \quad (13)$$

## V. Configurations of the Optimized Scenarios

The ATB simulation provided 500 dispersed LAV separation points and the one nominal LAV separation point for each of the following three scenarios: transonic, maximum dynamic pressure, and maximum dynamic pressure with Ares I nozzle failure. The LAV initial conditions provided by the ATB simulation are the position, velocity, attitude, attitude rate, atmosphere, and wind. Each of the 500 dispersed LAV separation points was used in the ANTARES LAV simulation four times, with differing mass properties and aerodynamic uncertainties. The mass properties and aerodynamic uncertainties were held constant between the baseline and optimized configurations. The atmosphere data and winds throughout each LAV simulation used the ATB atmosphere and winds profile from the initializing ATB trajectory. For each scenario, the baseline configuration was the standard Orion production gains schedule. The gains schedule for each of the optimized configurations was generated using the method of steepest descent as described in the section “Method of Gains Optimization,” above.

## VI. Trajectory Results

The performance of the gains schedule was evaluated using the ANTARES simulated environment through a dispersion set of 2,000 runs and one nominal set. The performance metric was how closely the nominal and off-nominal  $\alpha$  profiles matched the desired  $\alpha$  profile. The runs with the optimized gains schedule were compared to the runs with the Orion production gains schedule, which was the baseline. The evaluation was limited to the ascent portion of the abort trajectory up to reorientation. For each of the three scenarios the nominal, mean, mean  $\pm 3\sigma$ , and the number of tumbling cases was compared. The mean and mean  $\pm 3\sigma$  profiles were created by evaluating the  $\alpha$  probability density function at each time point for the runs that did not tumble. Figure 4 shows a sample histogram and probability density function of the transonic scenario at 7 s after abort. The comparison of the profiles was performed by summing the magnitude of  $\alpha$  along the profiles and then differencing the optimized from the baseline. Any time the difference (delta) is greater than 0, the optimized trajectories were closer to the desired  $\alpha$  profile than the baseline trajectories.

The  $\alpha$  profiles for the baseline and optimized simulated transonic trajectories are provided in Fig. 5. The delta  $\alpha$  profiles are provided in Fig. 6. The trajectories that tumbled prior to reorientation were reduced from 217 in the baseline to 165 in the optimized, which is an improvement of 24.0 percent.

The  $\alpha$  profiles for the baseline and optimized simulated maximum dynamic pressure trajectories are provided in Fig. 7. The delta  $\alpha$  profiles are provided in Fig. 8. The trajectories that tumbled prior to reorientation were reduced from 272 in the baseline to 261 in the optimized, which is an improvement of 3.3 percent.

The  $\alpha$  profiles for the baseline and optimized simulated maximum dynamic pressure trajectories with Ares I nozzle failure are provided in Fig. 9. The delta  $\alpha$  profiles are provided in Fig. 10. The trajectories that tumbled prior to reorientation were reduced from 329 in the baseline to 176 in the optimized, which is an improvement of 46.5 percent.

Summary statistics of the difference between the baseline  $\alpha$  profiles and the optimized  $\alpha$  profiles are provided in Table 1.

**Table 1. Results summary for the optimized abort flight test scenarios angle of attack profiles compared to the baseline abort flight test scenarios angle of attack profiles.**

		Transonic, percent	Maximum dynamic pressure, percent	Maximum dynamic pressure with nozzle failure, percent
Nominal improvement	trajectory	49.0	56.9	34.8
Mean improvement	trajectory	5.2	28.3	36.8
Mean $\pm 3\sigma$ improvement	trajectory	45.1	61.4	59.7
Tumbling reduction		24.0	3.3	46.5

All of the scenarios involved showed improvement over the baseline  $\alpha$  profiles through the gains schedule optimization effort. The smallest improvements were in the mean trajectory in the transonic scenario, 5.2 percent, and the tumbling in the maximum dynamic pressure scenario, 3.3 percent. The greatest improvements were in the mean  $\pm 3\sigma$  trajectories of the maximum dynamic pressure scenario, 61.4 percent, and the maximum dynamic pressure with nozzle failure scenario, 59.7 percent. The greatest overall improvement was in the maximum dynamic pressure scenario with an Ares I nozzle failure, which are initialized at large values  $\alpha$  and  $q$ .

## VII. Conclusion

The error between the optimized angle of attack profiles and the desired angle of attack profile was reduced from the error of the baseline angle of attack profiles. The method of steepest descent is effective for tuning the gains schedule of the Orion ascent abort flight tests. All three of the analyzed scenarios benefitted from tailoring the gains schedule to the specific flight-test conditions. Based on the improvements resulting from the gains schedule optimization efforts, it is recommended that the Orion ascent abort flight tests use an individually-optimized set of gains. Future versions of the launch abort system controller can reduce the errors from the desired angle of attack profile by implementing a two-dimensional gains schedule with Mach number or altitude as the second dimension. This method would allow the production controller the ability to use gains schedule that were tuned for a variety of ascent abort scenarios.

## References

- <sup>1</sup>Davidson, J., Madsen, J., Proud, R., Merritt, D., Raney, D., Sparks, D. et al., "Crew Exploration Vehicle Ascent Abort Overview," AIAA 2007-6590.
- <sup>2</sup>Burden, R. L., and Faires, J. D., *Numerical Analysis*, 7<sup>th</sup> ed., Wadsworth Group, Brooks/Cole, Pacific Grove, California, 2001.

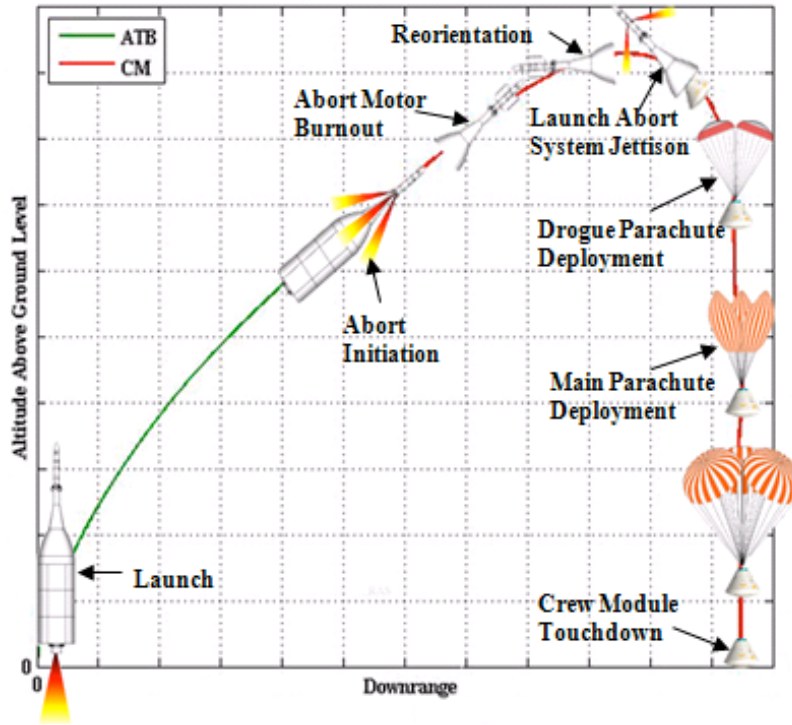


Figure 1. Sequence of events for an aborted Orion launch.

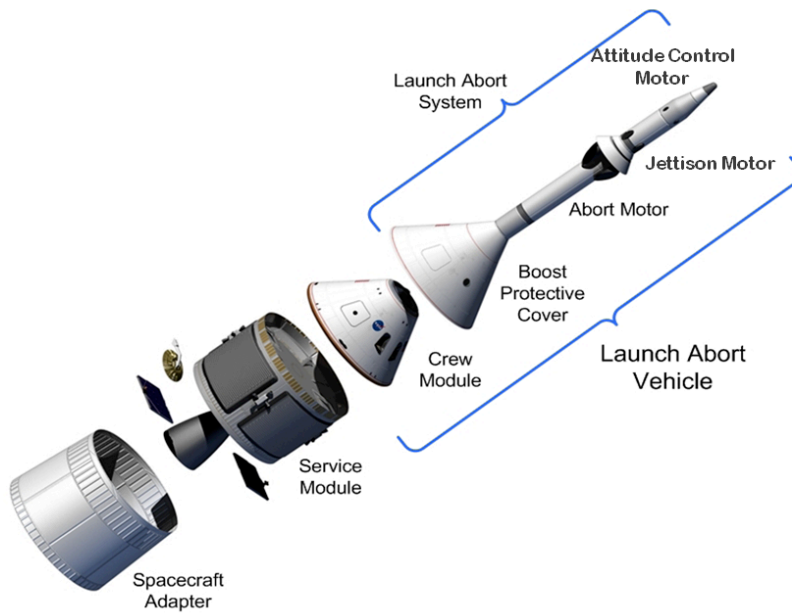


Figure 2. Orion vehicle breakdown and naming convention.<sup>1</sup>

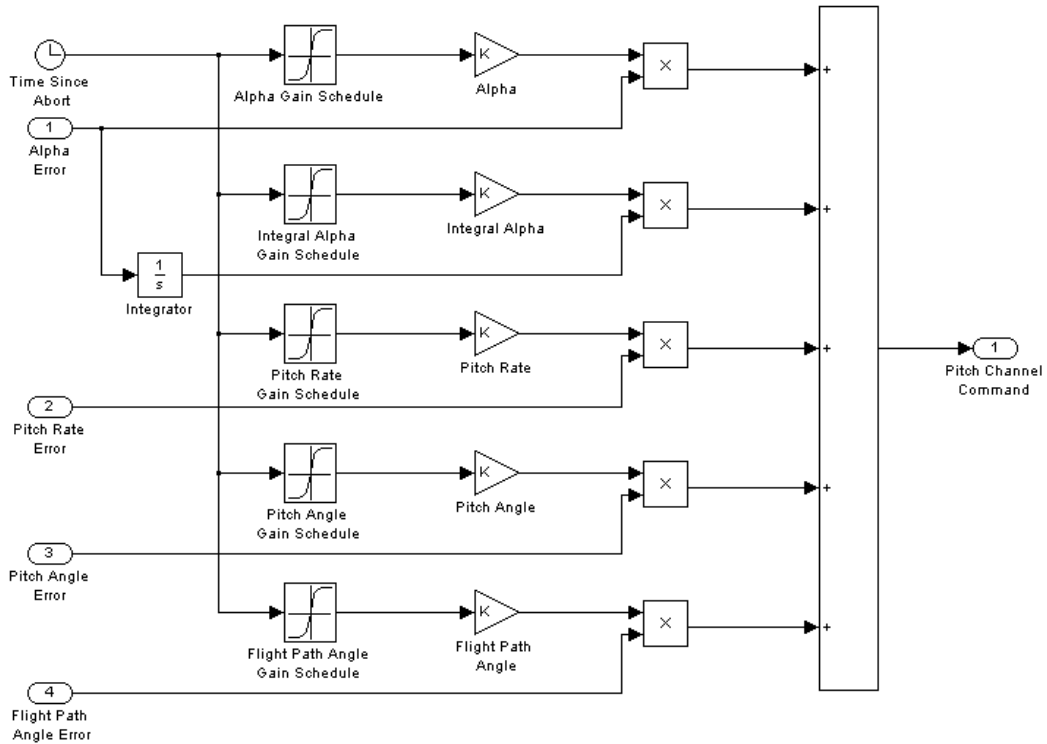


Figure 3. Block diagram of the Launch Abort System controller pitch channel.

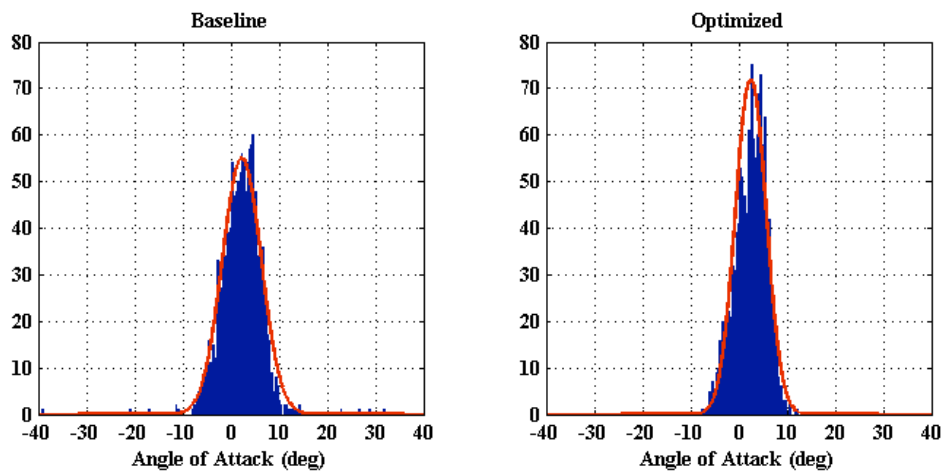


Figure 4. Histograms of the angle of attack at 7 s after abort for the transonic ascent Abort Flight Test.

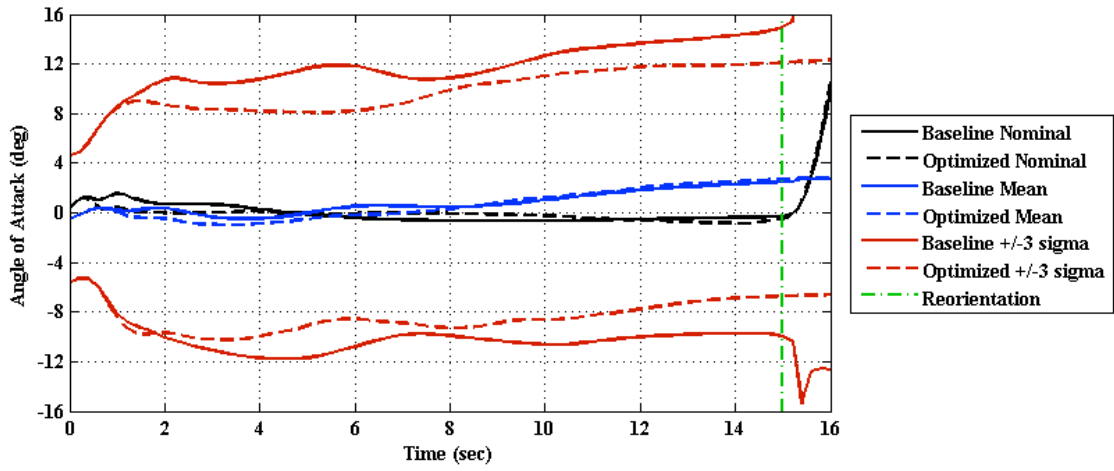


Figure 5. Angle of attack profiles for the transonic ascent Abort Flight Test.

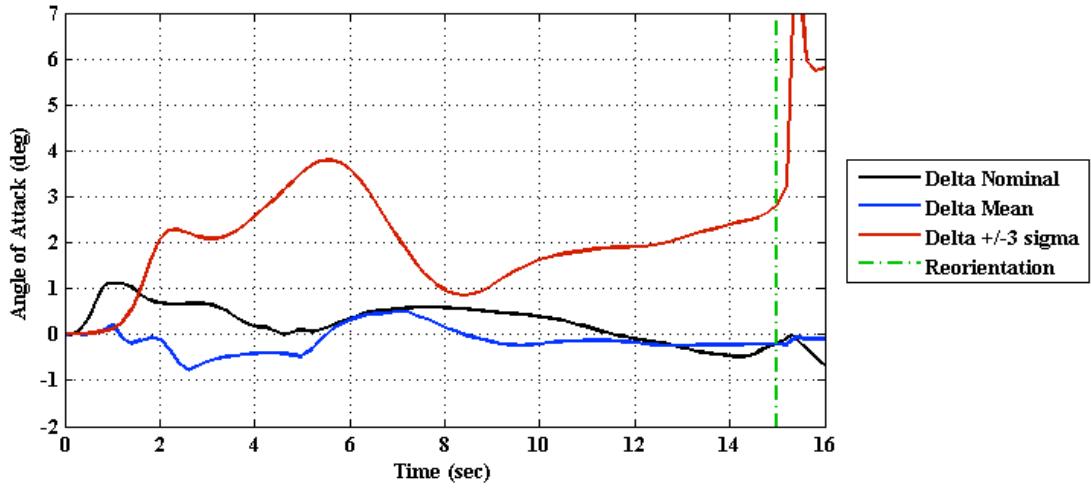


Figure 6. Delta angle of attack profiles for the transonic ascent Abort Flight Test.

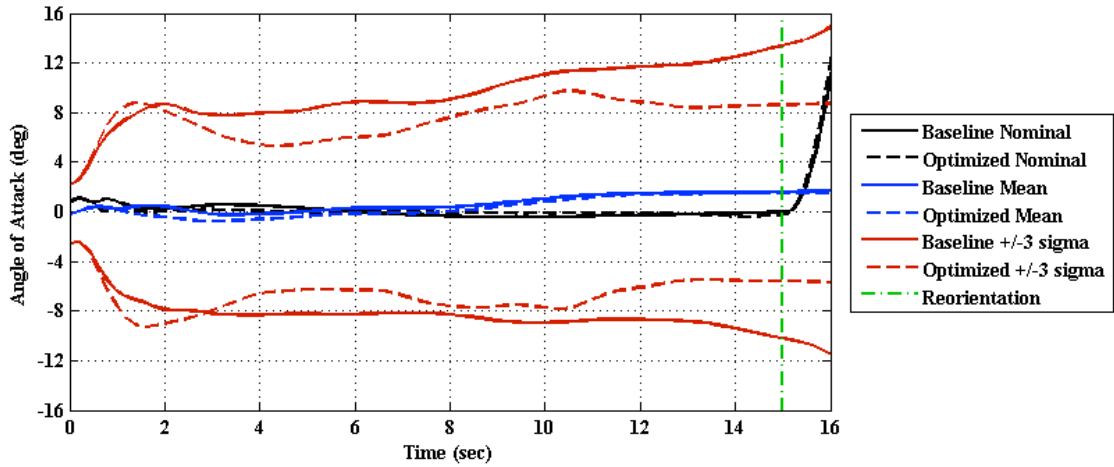


Figure 7. Angle of attack profiles for the maximum dynamic pressure ascent Abort Flight Test.

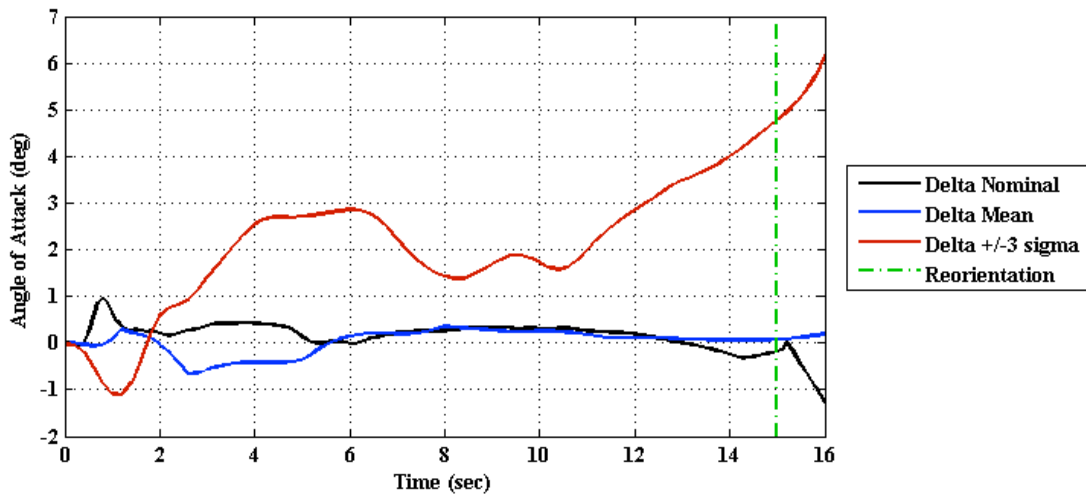


Figure 8. Delta angle of attack profiles for the maximum dynamic pressure ascent Abort Flight Test.

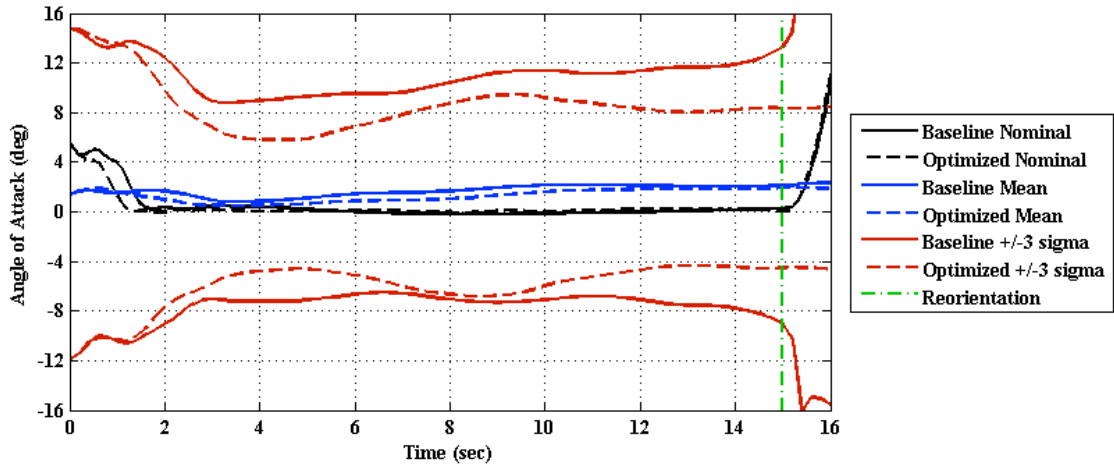


Figure 9. Angle of attack profiles for the maximum dynamic pressure with nozzle failure ascent Abort Flight Test.

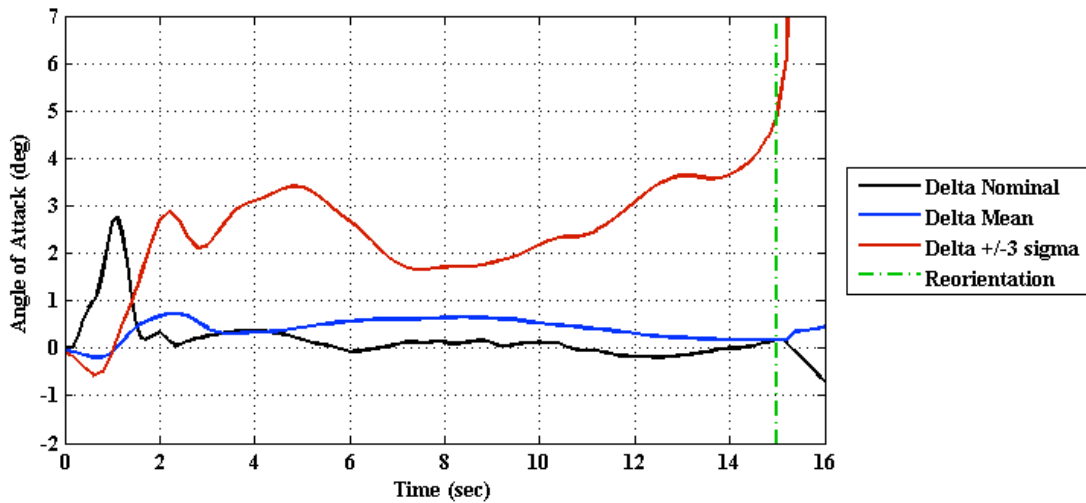


Figure 10. Delta angle of attack profiles for the maximum dynamic pressure with nozzle failure ascent Abort Flight Test.